

This article was downloaded by:

On: 25 January 2011

Access details: *Access Details: Free Access*

Publisher *Taylor & Francis*

Informa Ltd Registered in England and Wales Registered Number: 1072954 Registered office: Mortimer House, 37-41 Mortimer Street, London W1T 3JH, UK



Separation Science and Technology

Publication details, including instructions for authors and subscription information:

<http://www.informaworld.com/smpp/title~content=t713708471>

Fluid Stabilization during Isoelectric Focusing in Cylindrical and Annular Columns

N. B. Egen^a; G. E. Twitty^a; W. Thormann^a; M. Bier^a

^a CENTER FOR SEPARATION SCIENCE UNIVERSITY OF ARIZONA, TUCSON, ARIZONA

To cite this Article Egen, N. B. , Twitty, G. E. , Thormann, W. and Bier, M.(1987) 'Fluid Stabilization during Isoelectric Focusing in Cylindrical and Annular Columns', *Separation Science and Technology*, 22: 5, 1383 — 1403

To link to this Article: DOI: 10.1080/01496398708058406

URL: <http://dx.doi.org/10.1080/01496398708058406>

PLEASE SCROLL DOWN FOR ARTICLE

Full terms and conditions of use: <http://www.informaworld.com/terms-and-conditions-of-access.pdf>

This article may be used for research, teaching and private study purposes. Any substantial or systematic reproduction, re-distribution, re-selling, loan or sub-licensing, systematic supply or distribution in any form to anyone is expressly forbidden.

The publisher does not give any warranty express or implied or make any representation that the contents will be complete or accurate or up to date. The accuracy of any instructions, formulae and drug doses should be independently verified with primary sources. The publisher shall not be liable for any loss, actions, claims, proceedings, demand or costs or damages whatsoever or howsoever caused arising directly or indirectly in connection with or arising out of the use of this material.

Fluid Stabilization during Isoelectric Focusing in Cylindrical and Annular Columns

N. B. EGEN, G. E. TWITTY, W. THORMANN, and M. BIER

CENTER FOR SEPARATION SCIENCE
UNIVERSITY OF ARIZONA
TUCSON, ARIZONA 85721

Abstract

The interest in fluid stabilization of focusing columns results from the attractive prospect of preparative isoelectric focusing as an alternative to chromatographic separations for downstream processing of proteins and peptides. In isoelectric focusing there is a variation of buffer composition, pH, conductivity, and temperature along the separation axis. The disturbing effects of the latter two parameters can be minimized using solid support media or gels. However, gravity-dependent convection and gravity-independent electroosmosis hamper focusing in free fluids in a complex way that prevents the scaling up of this process while maintaining the exquisite resolution of the analytical scale. The present study discusses methods for minimizing these disturbing effects in annular and cylindrical focusing columns of varying cross-sectional areas and internal geometries.

INTRODUCTION

Key factors in the design of electrophoretic instruments are convective fluid stabilization, temperature control, and sample detection. Poorer resolution is characteristic of all free solution electrophoretic separations not carried out in capillaries, thin fluid films, or with density gradient stabilization. Attempts to achieve complete separations in sharp or well-defined zones, predicted by theoretical considerations, are confounded by gravitationally induced convection, originating from sedimentation of denser particles and thermal gradients, as well as by gravity-independent electroosmosis (EO) (1-4). The disruptive influence of these effects is

suppressed in a successful separation. A microgravity environment should eliminate gravitationally induced convection, leaving the electrically driven convection, such as EO, as the major disturbing factor (1). Anticonvection stabilization can be achieved by entrapping the fluid in such matrices as cellulose acetate or gels (5). These inhibit convection by viscous shearing stress in the interstices of the fiber or molecular matrix. For analytical purposes, thin supporting matrices allow for effective cooling and the use of high potential gradients which result in short separation times (6). Polyacrylamide and agarose gels are considered to be the most effective media. For preparative isoelectric focusing (IEF) techniques, electrophoretic chambers can be stabilized against convection with cellulose powder, Sephadex, grains of plastic beads, and coherent or granulated gels of agar, agarose, starch, crosslinked polyacrylamide, and mixtures of agarose and polyacrylamide. The use of supporting media involves several inherent drawbacks from both theoretical and practical considerations. There is the possibility of interaction between sample and support. Electromigration of large particles, such as viruses, organelles, or whole cells, is impeded by the sieving effect of the supporting medium. Another disadvantage is that the supporting media can mask the sample detection during the experiment. IEF in free solution can alleviate some of these problems. It was first performed in instruments with several compartments, separated by membranes (7).

Stabilization of free fluid by its own viscosity is achieved in capillaries or in thin fluid films. The former methodology is employed in an analytical capillary apparatus, where either circular or rectangular separation troughs are used (8). Thin films are realized in devices with a free-flowing curtain (free-flow electrophoresis (9-11)). Such instruments are characterized by excellent resolution as long as the capillary diameter or the distance between the two parallel walls is smaller than 1 mm. Separations in larger cross-sectional areas or larger thicknesses of fluid layers require additional stabilization. A downward increase in density established by a concomitant concentration gradient of a polyol (such as sucrose) comprises the classical way of stabilizing free fluid (12-14). It also permits the simultaneous establishment of gradients of other parameters, such as pH and electrical conductivity. Various annular columns for this kind of electrophoresis are commercially available. Density gradient electrophoresis has disadvantages which are related to the presence of the polyol gradient. IEF patterns can vary with the medium; patterns in density gradients can be different than those in gels. Furthermore, fraction collection by elution from the bottom of the column decreases the resolution, and the removal of the density media can be tedious and devastating.

Valmet (15) introduced a process termed zone convection, using an apparatus with a series of parallel focusing trenches. Parallel ridges of the device's lid raise the fluid level within the trenches, causing electrical continuity for focusing. Removal of the lid separates the fractions defined by the trenches. Similar designs for zone convection IEF were reported from other laboratories (16, 17). U-tubes connected in series (17) or coils of PE tubing wound around a core of copper (18) were also constructed. After focusing, the coil was frozen and the fractions were isolated by cutting the tube in short sections. Alternatively, the closed U-tube approach was replaced by a horizontal glass coil apparatus having open ports on the top of each coil segment which permitted fraction collecting without destruction of the focusing chamber (19). The number of trenches, U-tubes, or coil segments determines the resolving capacity in zone convection IEF.

An ingenious solution was provided by Hjertén in which stabilization was obtained without a superimposed density gradient using rotation of a fluid about a horizontal axis to inhibit gravitationally induced movements (20, 21). Good separations were achieved in glass tubes of about 3 mm i.d. and rotation at 40 rpm. An approach to achieve fluid rotation by nonmechanical means was proposed by Kolin who used a radial magnetic field (22). His attempts failed for a horizontal tube but succeeded for an annular space of about 1.5 mm formed between two horizontal plastic cylinders of different diameters. Hjertén's and Kolin's principles are limited to tubes and annular spaces, respectively, with narrow diameters. Fluid stabilization by other means includes segmentation of the electrophoresis chamber into subcompartments with a parallel array of filters or membranes (23-25). It allowed a substantial increase of the internal diameter without considerable loss of resolution. The rotation about the horizontal axis may also be replaced by free flow or recycling of the fluid (11, 26).

The present paper compares methods for fluid stabilization in batch-wise IEF devices which were investigated during design stages of IEF columns for microgravity experiments aboard NASA's space shuttle. The studies were designed to determine the limitations of ground-based IEF in free solution. Monofilament nylon screens segmenting horizontal and vertical focusing columns with circular or annular cross sections, as well as impermeable plastic partitions, periodically occluding 30-60% of the cross-sectional area in circular columns, were tested and compared to results from an IEF capillary column with a rectangular cross section. The influence of the surface properties of cylindrical columns was also examined. The focusing dynamics of a pH 3.5-10 carrier ampholyte mixture and a three-component buffer mixture are discussed for the elucidation of the characteristics of the various assemblies.

MATERIALS AND METHODS

Three types of focusing cells were investigated. Their column lengths and solution volumes are: 1) Rotofor: 8.6 cm, 45 mL; 2) Flight Cell: 4.6 cm, 1.49 mL; and 3) CapScan: 10.0 cm, 0.06 mL. The Rotofor (25) is assembled with only one internal configuration, a compartmentalized, annular focusing chamber. The Flight Cell (Fig. 1) comprises a cylindrical focusing chamber which can be assembled in the various geometries depicted in Fig. 1(b) and with straight bore glass tubings of various internal diameters. The CapScan has a thin ribbonlike focusing trough (27).

i) The Rotofor (25) is a preparative scale, free solution IEF apparatus. It consists of a cylindrical cell of 8.6 cm length with a central glass cooling tube of 0.95 cm o.d., forming an annular focusing chamber with 5.7 cm² cross-sectional area. The gap between the two circular walls is 0.95 cm. A sample of about 45 mL focuses within 1–6 h at a power consumption of 10 W. Nineteen parallel, monofilament nylon screens (6 μ m pore, Tetko, Elmsford, New York) divide the focusing chamber into equally spaced, discrete compartments. The screens are bonded to silicone rubber supports (O-rings) which have protrusions at regular intervals to maintain proper spacing during assembly and operation. They also minimize electroosmosis. Rotation at 6.6 rpm around the focusing axis and the screens stabilize the fluid against convective disturbances. Ion-exchange membranes (Ionics, Watertown, Massachusetts) separate the focusing chamber from the electrode compartments. Access to each of the 20 subcompartments for sample loading and collection is through small inlet and outlet ports. Sample collection is extremely rapid and easily accomplished with an array of 20 needles which feed to test tubes contained in a vacuum box. In a modified version, the same apparatus was employed in a vertical mode (without rotation). Experiments were thermostated with recirculating cooling fluid having a temperature of about 5°C.

ii) The Flight Cell is a rectangular Plexiglas box, 9.5 \times 2.5 \times 2.5 cm, comprised of two subsections: a cylindrical IEF cell body and a nongassing anode compartment (Fig. 1a). A palladium disk with sufficient H₂-absorbing capacity for the duration of a single run is the cathode. The subsections are separated by a thin palladium foil electrode which is capable of recombining the oxygen produced at the anode of the focusing chamber with the hydrogen generated on its other side. The third electrode is silver, in 0.15 M NaCl. AgCl is produced upon current flow. The cylindrical focusing chamber with a length of 4.63 cm and an internal diameter of 0.64 cm (0.32 cm² cross section) can be

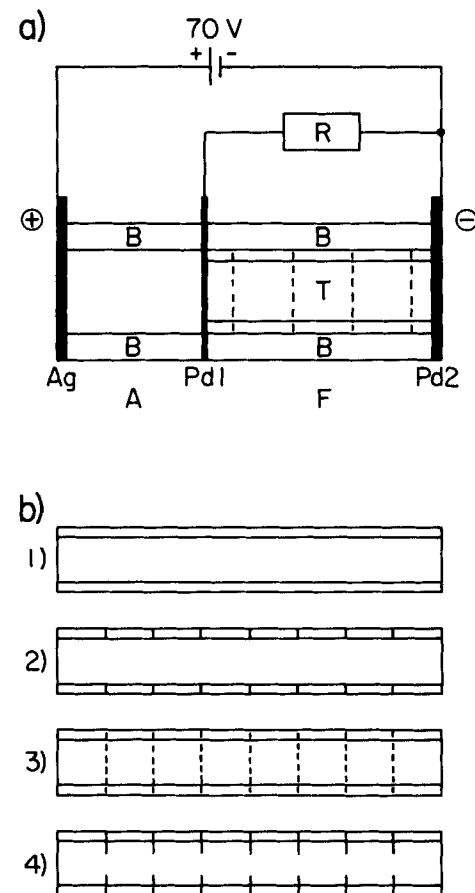


FIG. 1. (a) Schematic representation of the Flight Cell. A, anode compartment; F, focusing cell; T, focusing chamber (see b for configurations); B, Plexiglas body; Ag, silver anode; Pd1, platinized palladium foil cathode/anode; Pd2, platinized palladium cathode; R, shunt ($70\text{ k}\Omega$) ensures higher current in anode compartment compared to that in focusing cell. (b) Various configurations of the focusing chamber (T): (1) open glass tube; (2) glass rings separated by Mylar rings (0.1 mm) of i.d. identical to the glass; (3) nylon screens between glass rings; (4) Mylar rings with i.d. smaller than the glass between glass rings.

assembled with different internal arrangements for compartmentation (Fig. 1b). A completely open glass cylinder, plain or with an anti-electroosmotic coating, or a stack of 14 glass rings, represents the simplest arrangements. Another configuration is achieved by alternating glass rings with thin Mylar rings of identical cross section as the glass rings for periodic interruption of the glass wall within the cylindrical focusing space. A stack of alternating glass rings and monofilament nylon screens or alternating glass rings and thin Mylar disks, having a round hole in the center with a smaller internal diameter than that of the glass rings, are two other designs for column segmentation. These partitions can be introduced between adjacent or any number of glass rings, permitting the realization of different compartment lengths. Combinations of Mylar rings and screens were also investigated. To minimize density-driven convection in ground-based experiments, the whole cell was rotated around the focusing axis (typically about 6.6 rpm). Fractionation at 70 V occurs within about 1 h. Focusing was also tested in a vertical, stationary configuration. In a modified version the same cell body was assembled with cylindrical Pyrex focusing chambers having i.d.'s of 4.0, 3.3, and 2.3 mm. Rotation for those experiments was typically 14 rpm. The influence of rotational speed in the range of 0 to 100 rpm was also investigated. These experiments were carried out at room temperature.

iii) The CapScan apparatus in its IEF version (27) comprises a 10-cm capillary column with rectangular cross section (about 0.4×0.8 mm). Its lower wall is defined by a potential gradient array detector which monitors the electric field dynamics along the trough. The small dimension of the capillary enables sharp focusing in free solution. Dialysis membranes define both ends of the focusing column and isolate the electrode compartments from the trough. Focusing at 150 V was achieved in about 90 min (room temperature).

All three cell types were investigated with the same proteins and buffers. Blue stained (bromphenol blue) human serum albumin ($pI = 4.8$) and human hemoglobin ($pI = 7.3$) were focused in both a wide pH range system of carrier ampholytes (about 0.6% w/v) and a three-component buffer mixture. The composition of the two sample solutions is given in Table 1. All experiments commenced with a homogeneous mixture of carrier and test constituents. The focusing process was characterized by monitoring two parameters. First, the focusing current was measured under constant voltage or constant power (Rotofor). The comparison of the temporal behavior of the current as well as the ratio between initial and final (steady-state) currents were used to define the degree of focusing. Second, the two colored proteins in the sample were followed photographically. The effectiveness of fluid stabilization can be

TABLE I
Test Solutions for Focusing

(a) *Ampholine Solution (pH = 7.2; conductivity = 0.74 mS/cm)*^a

Ampholine pH range 3.5-10, 40% w/v	0.3 mL
Ampholine pH range 3.5-5, 40% w/v	0.2 mL
Ampholine pH range 5-7, 40% w/v	0.4 mL
NaOH, 0.1 M ^a	3.0 mL
Water	54.0 mL
HbA (as HbA.CO, 140 mg Hb/mL, 10 mM KCN)	1.0 mL
Alb (as Alb-blue, 225 mg/mL ^b)	0.15 mL

(b) *3-Component Buffer Solution (pH = 7.3; conductivity = 0.70 mS/cm)*

<i>p</i> -Amino benzoic acid	6 mM
Lysyl aspartic acid	10 mM
Arginine	8 mM
HbA (as HbA.CO, 140 mg Hb/mL, 10 mM KCN)	140 mg/50 mL solution
Alb (as Alb-blue, 225 mg/mL ^b)	33.75 mg/50 mL solution

^aA number of experiments were also performed without NaOH, having an initial pH and conductivity of 6.0 and 0.20 mS/cm, respectively.

^bAlbumin blue preparation: 0.9 mL human Alb (250 mg/mL) + 0.1 mL saturated bromophenol blue in 0.1 M NaOH.

judged by the sharpness of the transient double peak approach to equilibrium and the final distribution of the proteins. NaOH and phosphoric acid, 0.1 M each, were the respective cathodic and anodic electrolytes for the Rotofor and the CapScan apparatus. A DC Power Supply 2103 (LKB, Bromma, Sweden) was used with the Rotofor, and the other separation cells were powered with a Kepco Power Supply APH 2000M or a home-made voltage stabilized unit.

RESULTS AND DISCUSSION

Rotofor

An important consideration in the design of the Rotofor was the orientation of the focusing axis with respect to gravity. Several operating modes were explored including i) horizontal rotation, ii) horizontal oscillation (rocking), iii) horizontal stationary, and iv) vertical stationary. A typical example of a current-time relationship under constant voltage (790 V) together with the pH profile measured after fractionation is given

in Fig. 2(a). Current and voltage time profiles obtained under constant power (20 W), presented in Fig. 2, shows the difference between horizontal rotation (b) and horizontal nonrotation (c). The corresponding data are summarized in Table 2(a). The pH gradients obtained while rotating under constant voltage and constant power are essentially indistinguishable. However, when rotation is ceased (Fig. 2c) the pH gradient becomes slightly different from that of the horizontally

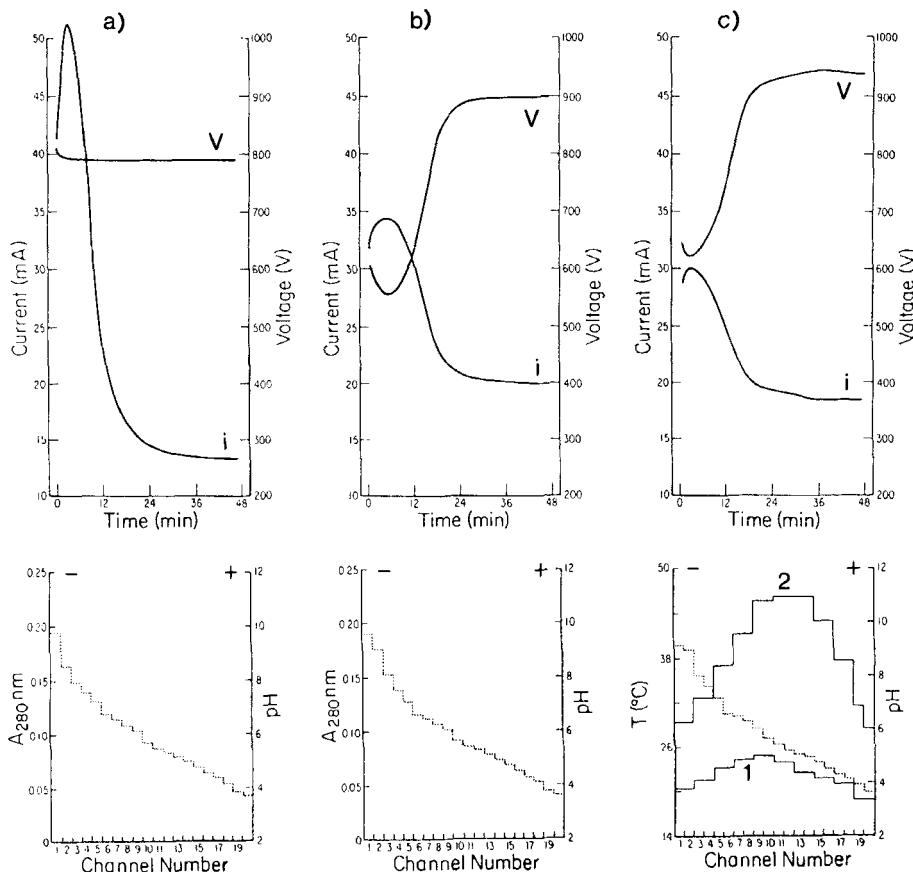


FIG. 2. Rotorfor: comparing operation at constant voltage (a: 790 V) vs constant power (b, c: 20 W); rotation (a, b) vs stationary (c). The three runs used identical focusing solution (Ampholine, Table 1) with a horizontal focusing axis. The panels present variation of voltage (V) and current (i) with time and show pH profiles along column axis at equilibrium (dotted line). It also presents the temperature distribution for the horizontal, nonrotating mode (c) measured at each outlet (1) and inlet (2) port.

TABLE 2
Conditions and Focusing Results

Column configuration	Column radius (mm)	Coating/ additive	Rotation ^a (rpm)	Current ratio ^b
<i>(a) Rotofor</i>				
1 Screen assembly	^c	None	6.6	3.33 ^d 2.40 ^e
2 Screen assembly	^c	None	No	2.27 ^e
3 Screen assembly	^c	None	Vertical	2.39 ^e
<i>(b) Flight Cell</i>				
1 13 Screen assembly	3.2	None	6.6	12.8
1' 5 Screen assembly	3.2	None	6.6	6.2
2 No partitions	3.2	None	6.6	2.5
3 No partitions	3.2	PVA	6.6	2.2
4 No partitions	3.2	Anti-EO coat	6.6	2.3
5 Glass rings only	3.2	None	6.6	2.2
6 Glass/Mylar rings	3.2	None	6.6	2.5
7 Mylar constrictors	3.2	None	6.6	9.7
<i>(c) Modified Flight Cell</i>				
1 No partitions	3.2	None	14	4.3
2 No partitions	2.0	None	14	8.3
3 No partitions	1.65	None	14	12.5
4 No partitions	1.15	None	14	13.0
<i>(d) CapScan</i>				
1 No partitions	^c	None	No	14.9

^aOr operation mode.

^bRatio of initial current and final current for the Ampholine system.

^cRotofor: 9.5 mm annular space; CapScan: 0.8 × 0.5 mm.

^dAt a constant 790 V.

^eAt a constant 20 W.

rotating cell and a significant temperature difference develops between the bottom (1) and top (2) of the focusing column. Focusing of the two proteins is poor in this configuration. It is clear that rotation improves cooling efficiency, permitting higher applied voltages. It also minimizes protein sedimentation. The combined effects result in a better resolution.

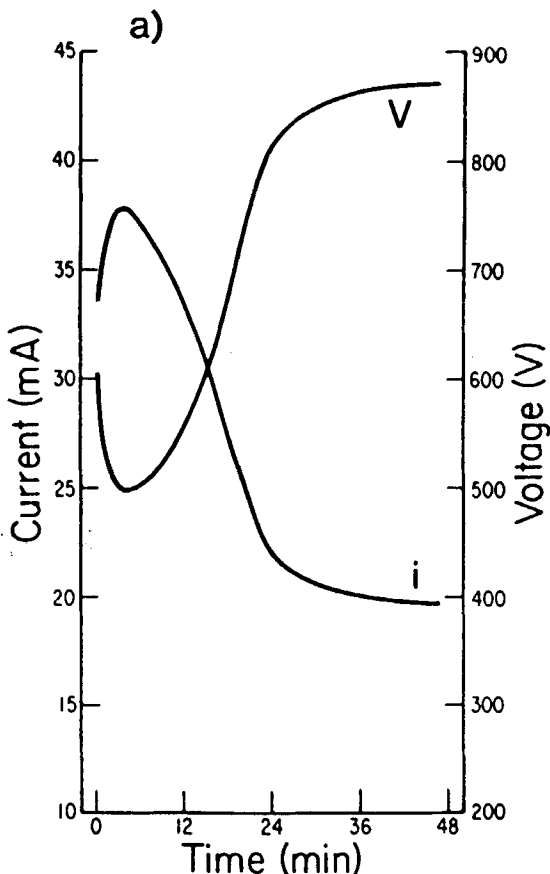
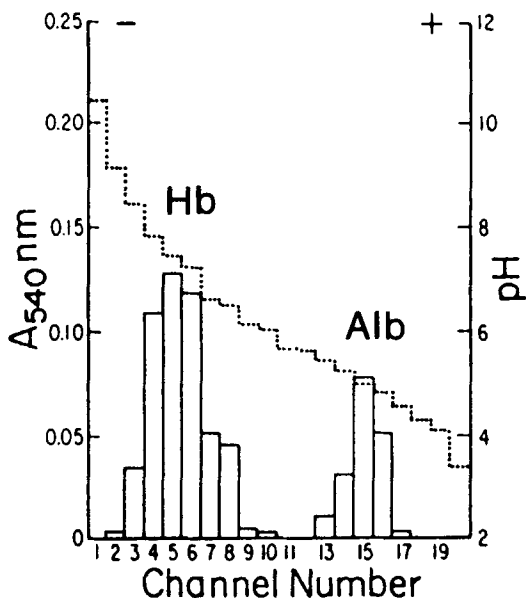


FIG. 3. Rotofor: comparing the operation in the vertical, stationary mode (a) with the horizontal, rotating mode (b) at constant power (20 W). The graphs depict the variation of voltage (V) and current (i) with time and present pH (dotted line) and absorbance at 540 nm (solid line) along the focusing axis at equilibrium. Ampholine solution without NaOH (Table 1) was used.



(a) II

Figure 3 (continued)

Figure 3 compares the operation in vertical orientation (a) with that of horizontal rotation (b) in otherwise identical conditions. Both current/voltage time profiles illustrate good focusing, achieved within 40 min. The absorbance of the fractions, determined at 540 nm, confirms the separations in both modes. It is evident from its steeper pH profile that the horizontal rotating mode is slightly better than the vertical mode. The vertical mode provided an unexpected high degree of stabilization as we expected thermal convection and protein sedimentation to penetrate the screens. Data obtained in the 3-component buffer system were essentially identical except that the proteins were focused within two segments. Experiments with the model system of hemoglobin and albumin have shown that small-angle oscillations are ineffective in preventing protein slumping. To maximize focusing efficiency, the cell must be rotated a minimum of 250° before reversing the direction, but this was still not comparable to that obtained with full rotation.

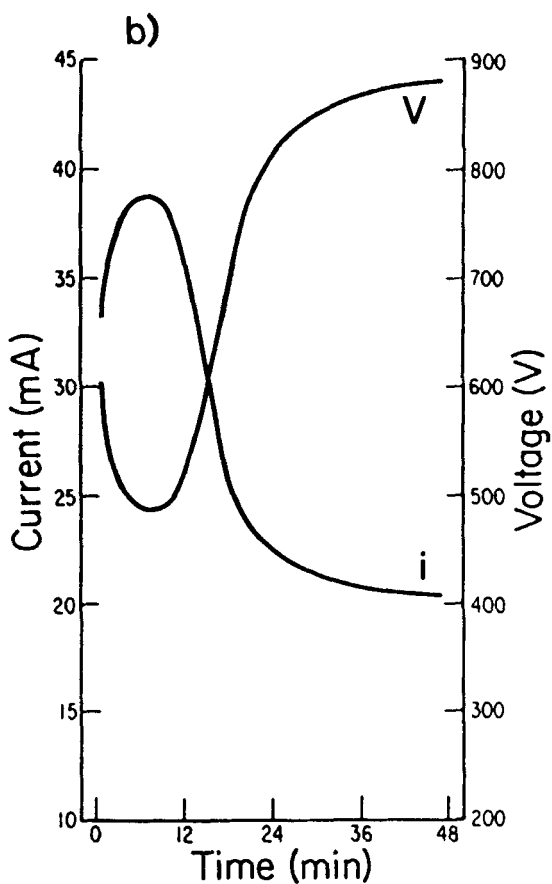
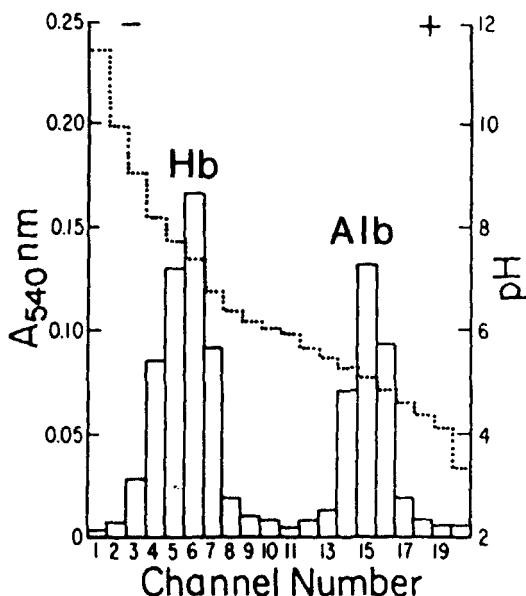


Figure 3 (continued)

Flight Cell

Ampholine focusing was performed in seven cells with various configurations (Table 2b) while rotating the cells around the column axis to approximate a microgravity environment. The first was a 14-compartment cell using nylon screens to define the sections. Of all configurations, this provided the best separation of the two proteins, as is seen in Fig. 4(a). The second is a completely open, one compartment cell using a single piece of glass tubing for the focusing chamber. This assembly depicts the other extreme of separation, Fig. 4(b). However, a decrease in focusing current could still be monitored (Table 2b, current ratio = 2.5). Experiments 3 and 4 were identical to the second one except for the presence of polyvinyl alcohol (PVA, 0.1% w/v) and antielectroosmotic



(b) II

Figure 3 (continued)

coating (28) on the column walls, respectively. The PVA was added in an attempt to coat the glass tube, reducing its surface charge and the effects of electroosmosis. The results were indistinguishable from those of Run 2. The other configurations, without achieving separation of the two proteins, included a focusing chamber consisting of 14 glass rings and one with glass rings separated by thin (100 μm) Mylar rings having congruent cross sections. The latter assembly was tested in order to evaluate the influence of a periodic interruption of the surface properties of the column wall. A respectable separation of albumin and hemoglobin occurred with 13 Mylar constrictors, as is depicted in Fig. 4(c). An identical set of experiments was performed using the simple buffer mixture. This system produces the same steady-state focusing patterns as does the Ampholine mixture in approximately 25% less time. These data are thus very similar to those presented in Fig. 4 and are not reproduced. Operation of the same configurations in a nonrotating, vertical mode was also tested, with good separation occurring only in the screen compartmented cell.

Table 2(b) presents a summary of the electrical current measured from rotating flight cells operated in various modes. Most notable is the comparison of the assemblies with (i) 13 nylon screens, defining 14

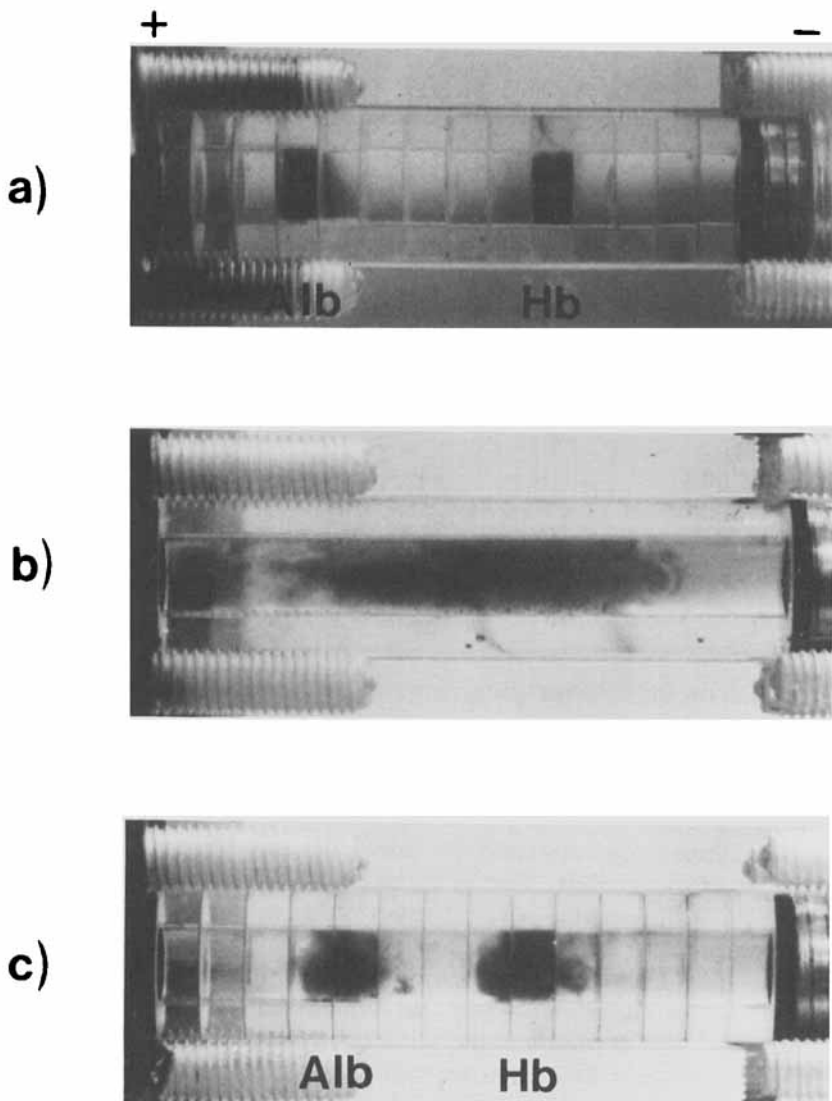


FIG. 4. Photographs of the Flight Cell at equilibrium. The focusing chambers are comprised of a cylinder, segmented with 13 nylon screens (a), a tube with no partitions (b), and a cylinder, segmented with 13 Mylar constrictors (c). Configurations (a) and (b) represent the extremes of resolving the two sample constituents. Ampholine solution (Table 1) was employed.

channels (1); ii) with 5 nylon screens, defining 6 compartments (1'); and iii) a single section provided by one glass tube (2). Plots of current vs time with Ampholine/protein in these cells, and for comparison one with buffer/protein, are presented in Fig. 5. These experiments demonstrate that the greater the number of compartments, within limits, the lower is the steady-state current produced. However, in an experiment (result not shown) with 140 compartments defined by the nylon screens, rather poor focusing with incomplete separation of the two test proteins was obtained.

Focusing of albumin and hemoglobin in the Ampholine system was also investigated in one segment cells with different column diameters. Rotation at 14 rpm was assumed to simulate a microgravity environment. Sharply focused bands were obtained in columns with diameters of 2.4

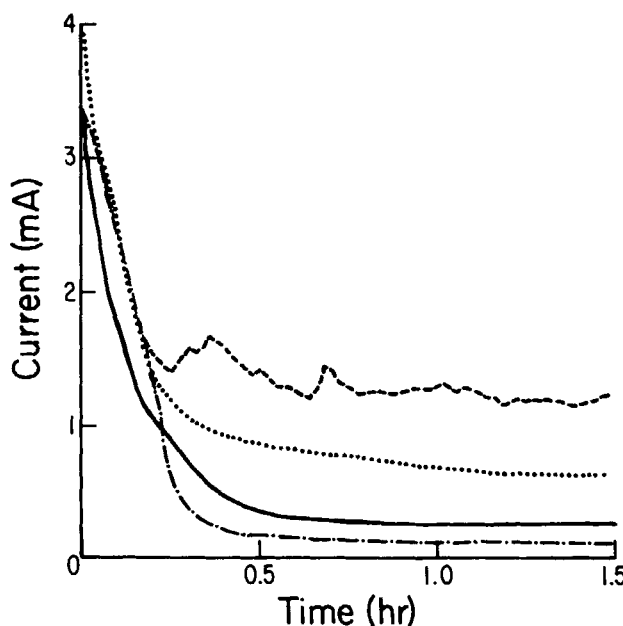


FIG. 5. Flight Cell: Focusing current variation with time with segment length as parameter using the Ampholine solution. The compartment length is varied by changing the numbers of glass segments between nylon screens. 1-Compartment, open tube (dashed line); 6-compartment (dotted line); 14-compartment (solid line). For comparison, the data of a 14-compartment cell with buffer solution (hybrid line) is shown. Good focusing and resolution is commensurate with a high initial to final current ratio and increased number of subcompartments.

mm with virtually no parabolic boundary profiles. Focusing gradually deteriorated with increasing diameter; no focusing being seen at 6.4 mm (Fig. 4b). This deterioration is due to gravity effects. It is difficult to discern the effects of EO in these columns. Experiments in space may be of decisive value in answering this question. The reason for the absence of parabolic boundary profiles in focusing is presently unclear, but is of crucial importance for design of continuous flow focusing instruments. A typical example of the variation of current with time, focused at constant voltage (70 V), is presented in Fig. 6. The results from the various columns are summarized in Table 2(c). They clearly reveal the impact of the column diameter on the stabilization of the fluid as expressed by an increase of the initial to final current ratio with decreasing column radius. After equilibrium was reached, the rotation was interrupted for a short time to allow sedimentation (slumping) of the focused protein samples to occur. The typical current increase and the establishment of a new equilibrium state during such a process is illustrated in the current-time profile. Finally, rotation was resumed and the system reequilibrated to its original steady state. This experimental procedure produced similar results with tubes of various i.d.'s (Table 2c), the larger tubes being

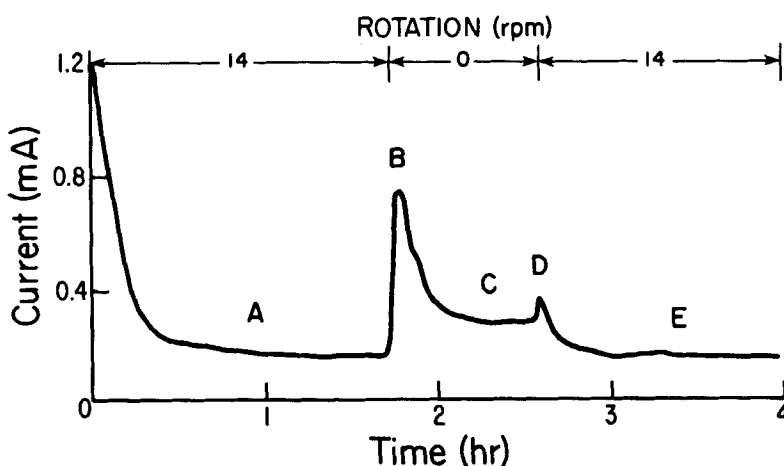


FIG. 6. Ampholine solution in Flight Cell with plain glass tube having an i.d. of 4 mm. The applied voltage was 70 V. Focusing occurred while rotating at 14 rpm until a steady state was maintained (A). At 1.7 h, rotation was ceased. The current briefly increased (B), then decreased to a new but higher steady state (C). At 2.6 h, rotation at 14 rpm was resumed, and after a brief rise in current (D), the original equilibrium current (E) was reestablished.

characterized with increasing noise due to increased solution turbulence. Photographs of focused (a) and slumped (b) proteins are shown in Fig. 7.

The influence of the rotating speed on the focusing process was also investigated using the Flight Cell assemblies. Steady-state currents at 2 to 8 rpm were found to be higher than at 14 rpm, as was expected. On the other hand, experiments with high-speed rotation in the order of 100 rpm were also characterized by a poorer performance because of an appreciable centrifugal effect. This was especially pronounced in the cell compartmented with Mylar constrictors. The rotating speed for a given column is strongly related to the diameter of the separation space and to a lesser extent to the method of segmentation. The larger the column diameter, the smaller the optimal rotational speed. It is interesting to note

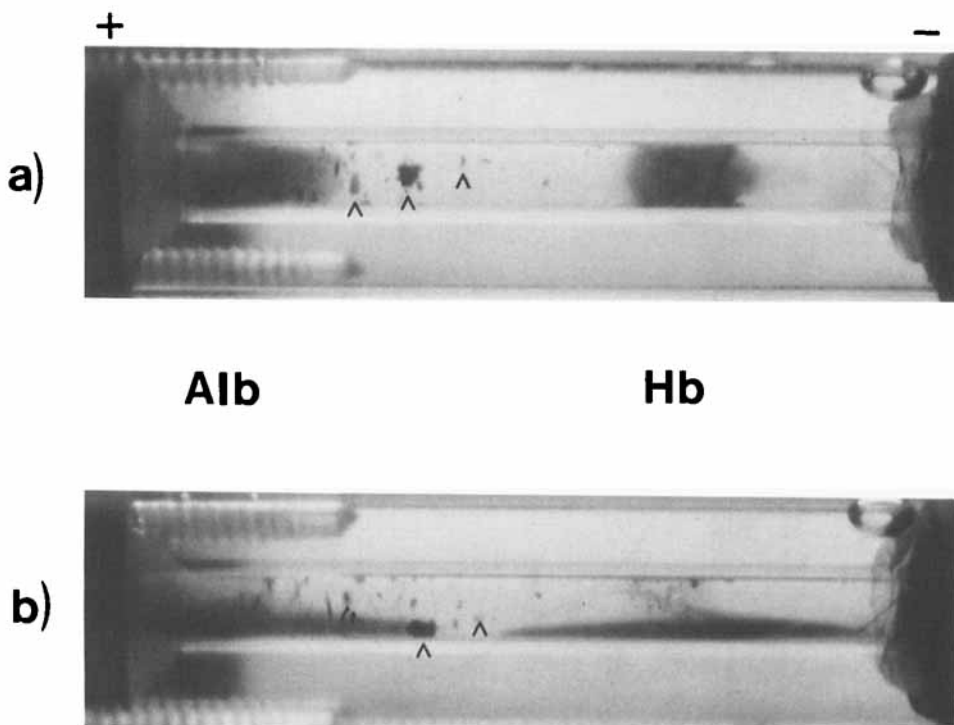


FIG. 7. Photographs of the Flight Cell with plain glass tube having an i.d. of 3.3 mm. The applied voltage was 70 V and focusing occurred with rotation at 14 rpm. (a) Equilibrium with rotation; (b) protein slumping after rotation was ceased. The arrowheads indicate denatured protein.

the consistency between our results (6.6 rpm for Rotofor and 14 rpm for Flight Cell) and that of Hjertén who found an optimal revolving speed of 40 rpm for a column radius of 1.5 mm (20).

CapScan

The experiments performed with the CapScan apparatus provide a comparison to a system in which convective disturbances are minimized without segmentation or rotation. Figure 8 presents the temporal behavior of the current for the Ampholine system, and the corresponding current ratio is listed in Table 2(d). The applied voltage was a constant 75 V. The current decreases substantially as focusing progresses. This is consistent with the monitored dynamics of the electric field profiles reported previously (29).

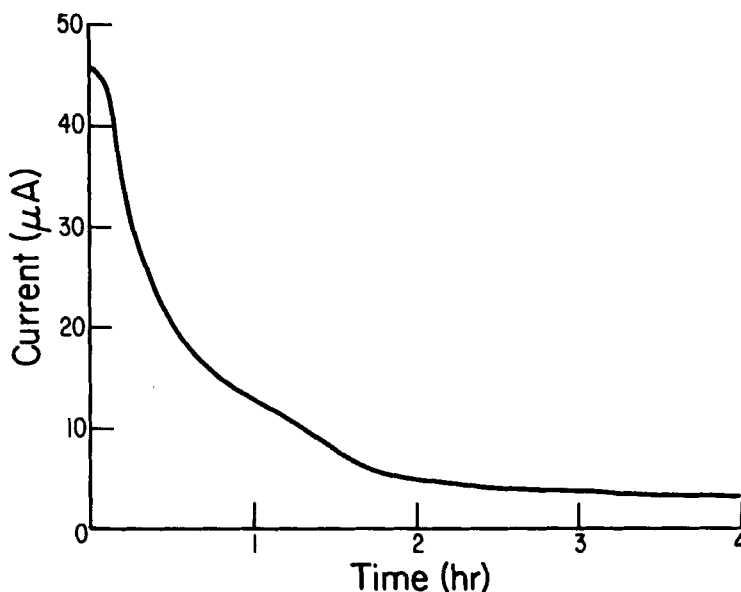


FIG. 8. CapScan: Focusing current as function of electrolysis time for the Ampholine solution. The applied voltage was 75 V.

CONCLUSIONS

The experiments described in this paper provide new insight into important aspects of fluid stabilization during free-fluid IEF which are extremely valuable for the evolution of this high resolution principle into the preparative scale. The degree of focusing (or fluid stabilization) in a given column can be expressed by the ratio between initial and final current. The higher this value, the better the resolution of the column. Low column cross-sectional areas result in good focusing. Rotating tubes with 3 mm i.d. or less and nonrotating tubes with less than 1 mm i.d. require no further stabilization. IEF on a larger scale, however, requires larger column dimensions in order to cope with the high throughput. The influence of rotation around the column axis only allows a modest increase of the focusing column volume.

Monofilament nylon screens for segmenting the focusing cell are especially useful for stabilizing fluid during electrofocusing by confining convection within the subcompartments. Their use also permits focusing in vertical columns of both circular and annular cross sections without density gradient stabilization. The selection of the 6 μm pore size screen material employed in this study was based upon previous investigations with our recycling IEF apparatus (26). It was found with this apparatus that pore sizes of 1 to 8 μm yield good separations. With increasing pore size, however, there is increasing convective mass transport across the screens. A pore size of 27 μm is significantly poorer. Electroosmotic pumping across those elements was found to be significant with the small pore sizes of 1 to 2 μm (fine particulates become trapped) but minimal at 6–10 μm . Other materials for compartmentation, such as dialysis membranes, PVC, Teflon, PAG, or PAG/agarose filters, induced an undesired, selective transport of components across those elements (this resulting in disturbing electroosmotic pumping), or had insufficient mechanical stability. The first phenomenon is based upon the unavailability of totally neutral materials. Flow tight plastic (Mylar) partitions, covering 30–60% of the cross-sectional area, as investigated in this work, represent an interesting alternative to the nylon screens but are less suitable for fluid stabilization. The studies show that the high resolution achieved with gels is not obtained with compartmentation of free solution.

Cylindrical and annular focusing columns in actual use allow protein fractionating rates in the order of 1 g/day. A capacity increase is clearly possible, as was shown by Jonsson and Rilbe (24) using a rotating, PVC-membrane compartmented electrolyzer with a circular cross-sectional area of 122 cm^2 , but effective cooling and compartmentation in such a

device appears to be demanding. The use of the nylon screens in a scaled-up version of our Rotofor is currently under investigation. Whether a true production scale is achievable in such a configuration will be reported in due course. The alternate avenue of employing continuous flow or recycling IEF devices (11) has recently emerged with the prospect of providing the capacity needed for downstream processing of fermentation products. Having small samples, however, does not justify the purchase of a fairly expensive apparatus. IEF devices, such as the Rotofor, with high resolution and low cost are the instruments of choice for this demand.

Acknowledgments

The authors would like to express their gratitude to Dr R. S. Snyder, NASA Marshall Space Flight Center, Huntsville, Alabama, for supplying the anti-electroosmotic coated glass tubes and for NASA's cooperation in developing the Flight Cell. This work was supported in part by NASA grants NSG-7333 and NAGW-693 as well as by NASA contact NAS8-32950.

REFERENCES

1. M. Bier, N. B. Egen, R. A. Mosher, and G. E. Twitty, in *Materials Processing in the Reduced Gravity Environment of Space* (G. E. Rindone, ed.), Elsevier, Amsterdam, 1982, p. 261.
2. Z. Deyl, *Electrophoresis: A Survey of Techniques and Applications, Part A: Techniques* (Journal of Chromatography Library, Vol. 18A), Elsevier, Amsterdam, 1979.
3. P. G. Righetti, C. J. van Oss, and J. W. Vanderhoff, *Electrokinetic Separation Methods*, Elsevier, Amsterdam, 1979.
4. P. G. Righetti, *Isoelectric Focusing: Theory, Methodology and Applications*, Elsevier Biomedical, Amsterdam, 1983.
5. B. Janik and J. Ambler, in *Electrophoresis '83* (H. Hirai, ed.), Walter de Gruyter, Berlin, 1984, p. 481.
6. A. Goerg, W. Postel, and R. Westermeier, *Anal. Biochem.*, 89, 60 (1978).
7. R. R. Williams and R. E. Waterman, *Proc. Soc. Exp. Biol. Med.*, 27, 56 (1929).
8. W. Thormann, R. A. Mosher, and M. Bier, in *Chemical Separations, Vol. I. Principles* (C. J. King and J. D. Navratil, eds.), Litarvan Literature, Denver, 1986, p. 133.
9. K. Hannig, *Electrophoresis*, 3, 235 (1982).
10. H. Wagner and R. Kessler, *GIT Lab.-Med.*, 7, 30 (1984).
11. M. Bier, N. B. Egen, G. E. Twitty, R. A. Mosher, and W. Thormann, in *Chemical Separations, Vol. I. Principles* (C. J. King and J. D. Navratil, eds.), Litarvan Literature, Denver, 1986, p. 153.
12. H. Svensson, *Arch. Biochem. Biophys. Suppl.*, 1, 132 (1962).
13. A. Kolin, *Proc. Natl. Acad. Sci.*, 41, 101 (1955).

14. N. Catsimpoolas, *Sep. Sci.*, **6**, 435 (1971).
15. E. Valmet, *Sci. Tools*, **16**, 8 (1969).
16. W. D. Denckla, in *Electrofocusing and Isotachophoresis* (B. J. Radola and D. Graesslin, eds.), Walter de Gruyter, Berlin, 1977, p. 423.
17. R. Quast, in *Electrokinetic Separation Methods* (P. G. Righetti, C. J. van Oss, and J. W. Vanderhoff, eds.), Elsevier, Amsterdam, 1979, p. 221.
18. J. Bours, in *Isoelectric Focusing* (N. Catsimpoolas, ed.), Academic, New York, 1976, p. 209.
19. R. Quast, in *Electrofocusing and Isotachophoresis* (B. J. Radola and D. Graesslin, eds.), Walter de Gruyter, Berlin, 1977, p. 455.
20. S. Hjertén, in *Methods of Protein Separation*, Vol. 2 (N. Catsimpoolas, ed.), Plenum, New York, 1976, p. 219.
21. P. Lundahl and S. Hjertén, *Ann. N. Y. Acad. Sci.*, **209**, 94 (1973).
22. A. Kolin, *Proc. Natl. Acad. Sci.*, **46**, 509 (1960).
23. H. Rilbe, *Prot. Biol. Fluids*, **17**, 369 (1970).
24. M. Jonsson and H. Rilbe, *Electrophoresis*, **1**, 3 (1980).
25. N. B. Egen, W. Thormann, G. E. Twitty and M. Bier, in *Electrophoresis '83* (H. Hirai, ed.), Walter de Gruyter, Berlin, 1984, p. 547.
26. M. Bier, N. B. Egen, T. T. Allgyer, G. E. Twitty, and R. A. Mosher, in *Peptides: Structure and Biological Function* (E. Gross and J. Meienhofer, eds.), Pierce Chemical Co., Rockford, Illinois, 1979, p. 35.
27. W. Thormann, G. E. Twitty, A. Tsai, and M. Bier, in *Electrophoresis '84* (V. Neuhoff, ed.), Verlag Chemie, Weinheim, 1984, p. 114.
28. J. W. Vanderhoff, F. J. Micale, and P. H. Krumrine, *Sep. Purif. Methods*, **6**, 61 (1977).
29. W. Thormann, N. B. Egen, R. A. Mosher, and M. Bier, *J. Biochem. Biophys. Methods*, **11**, 287 (1985).

Received by editor July 25, 1986